

Supporting Information:

Visualising Electrochemical Reaction Layers: Mediated vs Direct Oxidation

*Junling Ma, Minjun Yang, Christopher Batchelor-McAuley, Richard G. Compton**

Department of Chemistry, Physical and Theoretical Chemistry Laboratory, University of
Oxford, South Parks Road, Oxford OX1 3QZ, UK

SI Contents

Section 1: Thin-layer cell design

Section 2: Microscope setup

Section 3: Theoretical Model

Section 4: Relation of concentration and intensity profile

Section 5: Extra factors

Section 6: Spectra of HPTS and PYTS

Section 7: Fluorescence Intensity profiles of PYTS

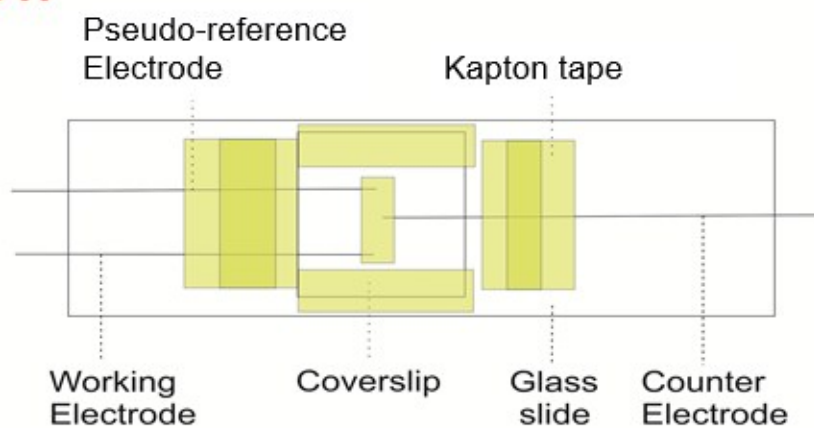
Section 8: Fluorescence Intensity profiles of HPTS

References

Section 1: Thin-layer cell design

Figure S1 displays the schematic of the thin-layer cell used which combine the electrochemical and optical measurements.

Top view



Side view

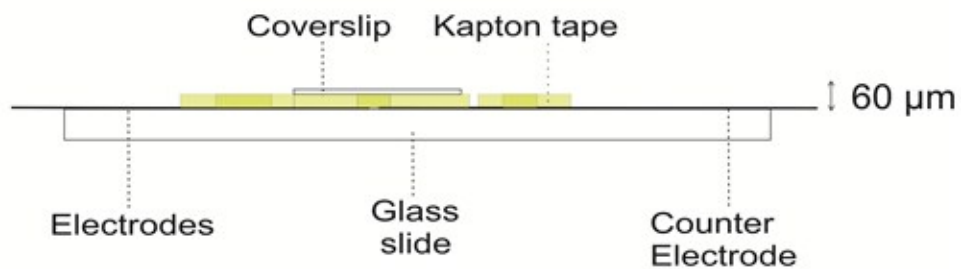


Figure S1: Thin-layer cell structure used for the opto-electrical measurements.

Section 2: Microscope setup

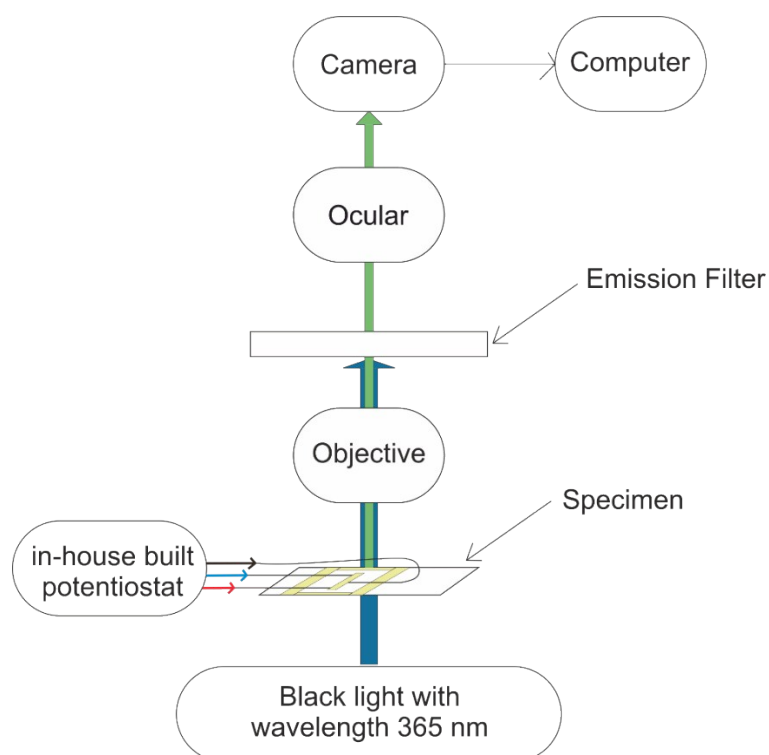


Figure S2: Schematic of the whole epi-fluorescent microscope setup.

The fluorescence excitation light source was provided by an EL Series Ultraviolet Hand Lamp with wavelength 365 nm (UVLS-24, Ultra-Violet Products Ltd., Upland, C.A., U.S.A.). Therefore, no further excitation filter and dichroic mirror are needed.

For the HPTS and PYTS experiment, MF530-43 and MF445-45 was used as the emission filter respectively.

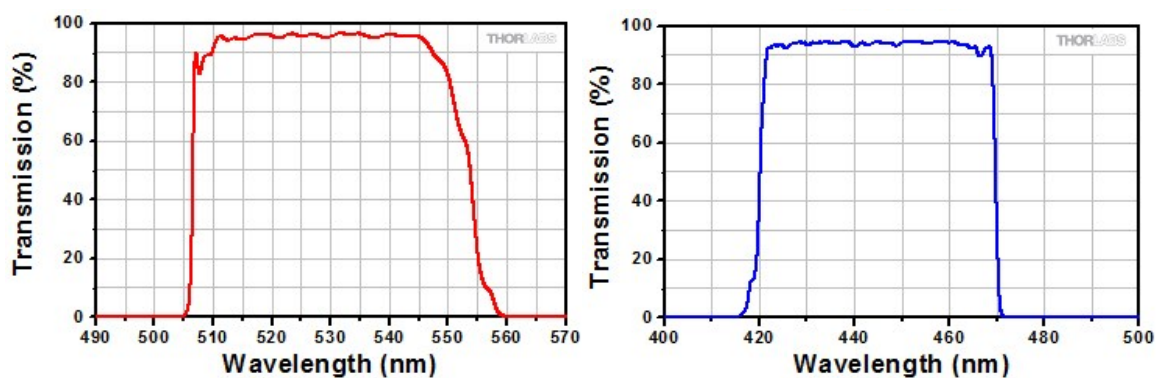


Figure S3: Emission filter transmission % for MF530-43 filter (left) and MF445-45 filter (right) provided by Thorlabs.

Section 3: Theoretical Model

In order to take account of the finite cell thickness, we use the Ln Tan cylinder coordinate system¹, which is applied for the simulation of a hemi-cylinder electrode in a thin layer cell. This coordinate system is used for simulation of both the direct and indirect oxidation reactions.

The Ln Tan cylinder coordinate system as two coordinates η and φ . The relationship between the Cartesian coordinates x and z is given by the following:

$$x/a = \frac{1}{\pi} \ln \frac{\sinh^2 \eta + \sin^2 \varphi}{\sinh^2 \eta + \cos^2 \varphi} \quad (1)$$

$$z/a = \frac{2}{\pi} \arctan \frac{\sinh 2\eta}{\sin 2\varphi} \quad (2)$$

where a is the cell height, and the figure below gives an example plot of this coordinate system.

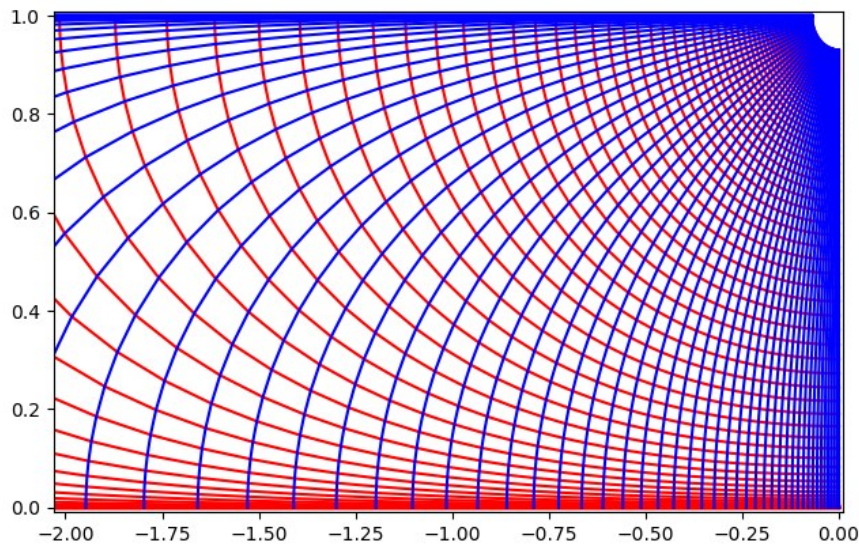


Figure S4: Ln Tan coordinates system: Red = equal η line, Blue = equal φ lines. $a = 1$, $\eta_0 = 1.45$ (electrode surface)

Variations in the concentration along the cylindrical axis is not considered consequently under this coordinate system.

$$\nabla C = \left(\frac{\pi}{4}\right) \sqrt{(\sinh^2(2\eta) + \sin^2(2\varphi))} \left[a_\eta \frac{\partial C}{\partial \eta} + a_\varphi \frac{\partial C}{\partial \varphi} \right] \quad (3)$$

and

$$\nabla^2 C = \left(\frac{\pi}{4}\right)^2 (\sinh^2 2\eta + \sin^2 2\varphi) \left[\frac{\partial^2 C}{\partial \eta^2} + \frac{\partial^2 C}{\partial \varphi^2} \right] \quad (4)$$

In the simulation we use an expanding in the x-direction perpendicular to the electrode, where near the electrode surface below a threshold X_s a dense grid is used and then expands at a rate proportional to γ :

$$\gamma_x = 5 \times 10^{-2}$$

$$X_s = 2 \times 10^{-6}$$

$$X[i] = X[i-1] + \gamma_x X_s \quad X < X_s \quad (5)$$

$$X[i] = X[i-1] + \gamma_x X[i-1] \quad X > X_s \quad (6)$$

Once these values of x have been found they are converted into values of η where $\varphi=0$. At distances greater than 2 an additional Cartesian grid is used. In φ a uniform grid spacing was used with 100 grid positions.

In this section, our theoretical models are presented in detail with the introduction of dimensionless parameters and plots.

Reaction





Dimensionless Parameters

Unit parameters	Interpretation	Dimensionless parameters
a (m)	Cell height	
L (m)	Length of the electrode	
x (m)	Space coordinate	$X = x/a$
z (m)	Space coordinate	$Z = z/a$
c (mM)	Concentration	$C_j = c_j/c_{A^*}$
D (m ² s ⁻¹)	Diffusion Coefficient	$d_j = D_j/D_A$
t (s)	Experimental time	$T = D_A t/a^2$
k ₁ (mol ⁻¹ m ³ s ⁻¹)	Bimolecular Second order rate constant	$K_1 = k_1 a^2 c_{A^*}/D_A$
k ₋₁ (s ⁻¹)	Unimolecular First Order rate constant	$K_{-1} = k_{-1} a^2/D_A$
k ₀ (m s ⁻¹)	Standard electrochemical rate constant	$K_0 = k_0 a/D_A$
E (V)	Electrode Potential	$\Theta = (E - E_f)F/RT$
v (V s ⁻¹)	Scan Rate	$\sigma = a^2 F v / D_A R T$
I (A)	Electrochemical Current	$J = I / L F D_A c_{A^*}$

Dimensionless equations

For the direct oxidation case only the diffusion equation for species A needs to be considered:

$$\frac{\partial C_A}{\partial T} = \nabla^2 C_A \quad (10)$$

For the indirect oxidation process we need to consider the concentrations of four different species, Y, Z, A and B. The dimensionless diffusion equations with the chemical terms are:

$$\frac{\partial C_Y}{\partial T} = d_Y \nabla^2 C_Y \quad (11)$$

$$\frac{\partial C_Z}{\partial T} = d_Z \nabla^2 C_Z - K_1 C_Z C_A + K_{-1} C_B \quad (12)$$

$$\frac{\partial C_A}{\partial T} = d_A \nabla^2 C_A - K_1 C_Z C_A + K_{-1} C_B \quad (13)$$

$$\frac{\partial C_B}{\partial T} = d_B \nabla^2 C_B + K_1 C_Z C_A - K_{-1} C_B$$

The electrode flux needs to be integrated across the electrode surface.

$$J_j = \nabla C \quad (14)$$

Under Ln-Tan cylindrical coordinates this becomes $J = \left(\frac{\pi}{4}\right) \sqrt{(\sinh^2(2\eta) + \sin^2(2\varphi))} \frac{\partial C}{\partial \eta}$ (15)

Numerical integration was achieved using a trapezoid rule and was used to assess the flux at the electrode interface. The following sum expresses the total electrode flux as a function of

$$J_{tot} = \frac{2r}{a} \sum_0^{\pi/4} \frac{J_j + J_{j-1}}{2} 2\Delta\varphi \quad (16)^{I=-FDcLJ_{tot}}$$

(17)

Figure S5 depicts the simulated optical response for two mechanisms in dimensionless format.

In the dimensionless form, the distance from the center of electrode, x-axis, equals the original

distance divided by the cell height. $X = x/a$, where a is the cell height. Dimensionless time is

$$T = D_A t / a^2$$

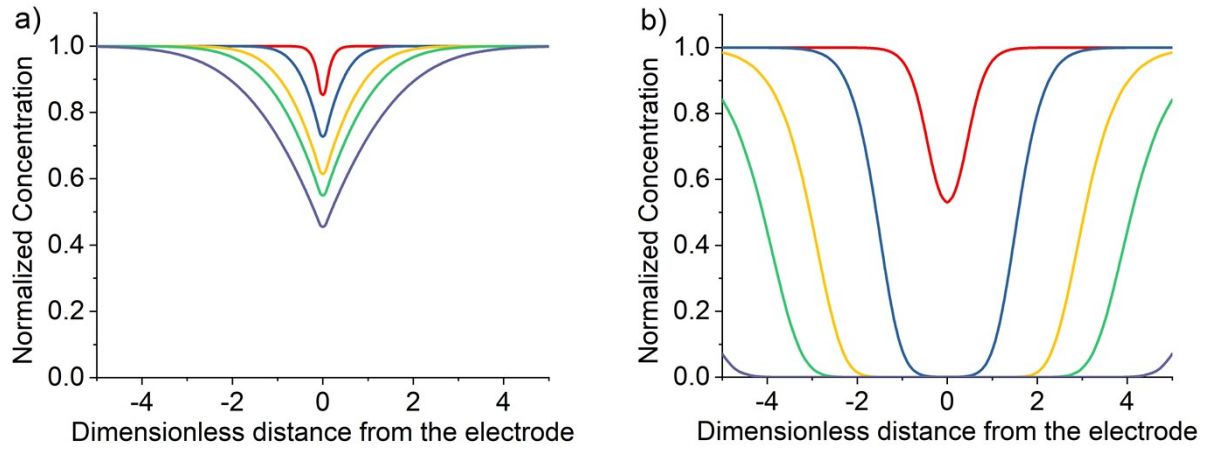


Figure S5: Dimensionless form of the simulated optical response for a) the direct and b) the indirect oxidation mechanism. Variation of the relative fluorescence intensity of species A as a function of distance perpendicular to the electrode as a ratio of the cell height. Plot of the variation in the profile as a function of dimensionless time $T = 0.25, 2.5, 7.5, 12.5$ and 25 simulated by Ln Tan.

Section 4: Relation of concentration and intensity profile

As mentioned in the main text that the normalized concentration profiles can mirror the fluorescence intensity profiles. In this section, the possible errors introduced by this model are discussed. In the simulation model, we measured the average concentration of the fluorophore in the z-direction. However, in reality the intensity we obtained from the microscope measures the light in a cone-like structure instead of the column. Figure S7 depicts the numerical aperture of a thin lens.

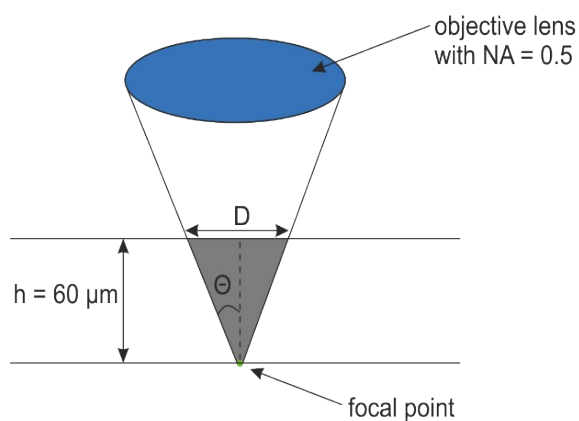


Figure S6: Numerical aperture of a thin lens.

Using the equations:

$$NA = n \sin(\theta) \quad (18)$$

$$D = 2h \tan(\theta) \quad (19)$$

with the numerical aperture, NA, equals 0.5, the index of refraction, n , of water is 1.33. h is the cell height of the thin-layer cell which is equal to $60 \mu\text{m}$. Therefore, D is equal to $48.7 \mu\text{m}$. Although the fluorescence intensity of more pixels is measured in reality, the error is minimised by the low resolution at out-of-focus positions. The resolution is not uniform through the whole cell due to the depth of field. The resolution of the top surface of the solution would be decreased by around 80% compare to that at the bottom focal point.

The Beer-Lambert Law:

$$A = \epsilon cl \quad (20)$$

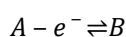
$$A = \log \frac{I_0}{I} \quad (21)$$

is used to calculate the intensity of the fluorophore at the top surface of the cell with a cell height of $60 \mu\text{m}$. From the UV-Vis absorbance spectra we got that the extinction coefficient of HPTS at 365 nm, the excitation wavelength used in the optical fluorescence experiment, is $11500 \text{ M}^{-1}\text{cm}^{-1}$. Length is equal to the cell height which is $60 \mu\text{m}$. The light intensity at the

surface layer of the solution is 0.98, 0.85 and 0.20 of the initial light intensity for HPTS with concentration of 0.1 mM, 1.0 mM and 10 mM respectively. Therefore, we can see that when the concentration is high, the light intensity is not uniform throughout the thin-layer cell. The normalization can minimise the error introduced by this non-unity. Also, at high concentration, the reaction does not take place as fast as at lower concentrations.

Section 5: Extra factors

For the one electron transfer oxidative reaction,



the shape of this profile will be independent of the used concentration of the fluorophore (shown in figure S6 (a)). Figure S6 (b) – (c) depicts the variation of the simulated fluorescence profiles as a function of the thickness of the cell and the radius of the electrode respectively.

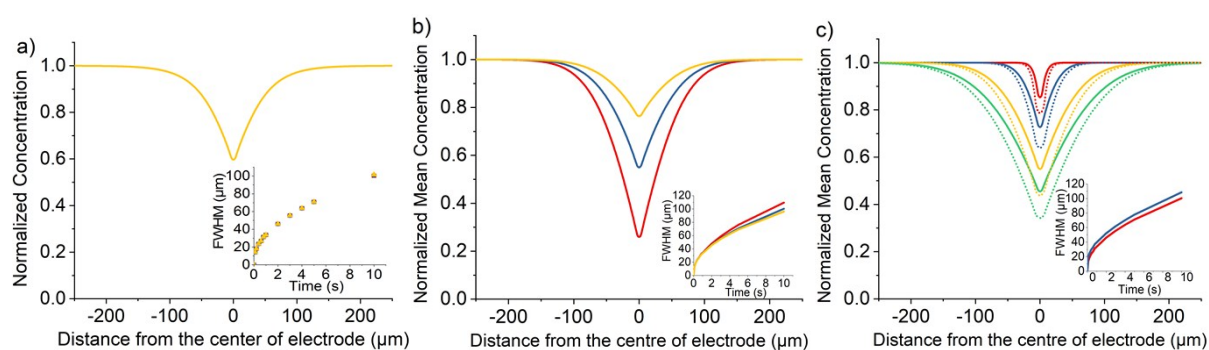


Figure S7: Simulated optical response for the direct oxidation mechanism. Variation of the relative fluorescence intensity of species *A* as a function of distance perpendicular to the electrode. a) The fluorescence intensity profile after 5 seconds as a function of the fluorophore concentration $[A]_{\text{bulk}} = 0.1 \text{ mM}$ (red), 1.0 mM (blue) and 10 mM (yellow). (Inlay) Plot of full-width half maximum of the concentration profile at $t = 0$ to 10 s . b) Plot of the variation in the profile at $t = 5 \text{ s}$ with the thickness of cell equals to $30 \text{ }\mu\text{m}$ (red), $60 \text{ }\mu\text{m}$ (blue) and $120 \text{ }\mu\text{m}$ (yellow); (inlay) plot of full-width half maximum of the fluorescence intensity profile at $t = 0$ to 10 s . c) Plot of the variation in the profile at $t = 0.1, 1, 5$ and 10 s with the radius of the working electrode, R , equals to $3.5 \text{ }\mu\text{m}$ (Solid lines) and $7.0 \text{ }\mu\text{m}$ (Dotted); (inlay) plot of full-width half maximum of the fluorescence intensity profile at $t = 0$ to 10 s .

Section 6: Spectra of HPTS and PYTS

The absorbance and fluorescence spectra for HPTS and PYTS are depicted in this section. The black line is the absorbance spectrum and the red line is the normalized fluorescence intensity.

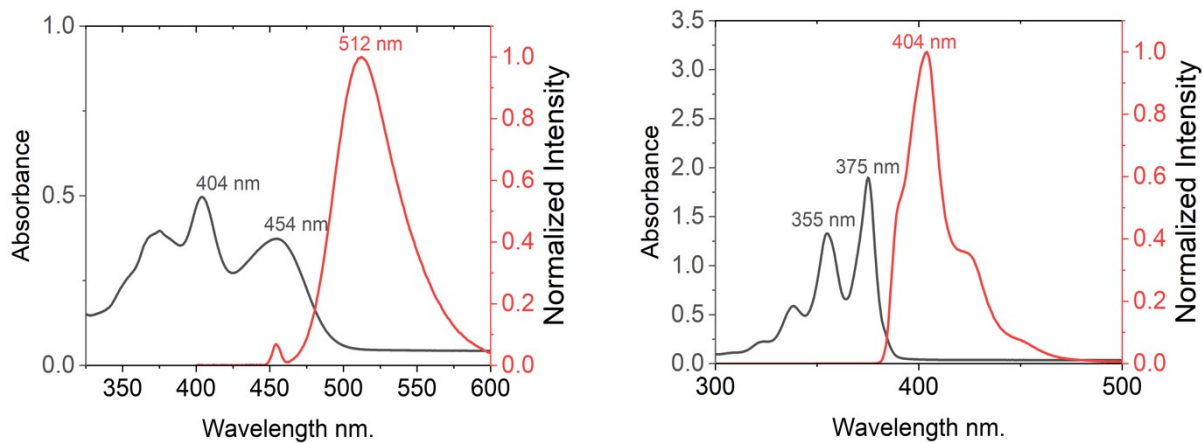


Figure S8: UV-Vis absorbance and fluorescence emission spectrum of 31.25 μM HPTS (left) and 31.25 μM PYTS (right) in pH 7 phosphate buffer solution with 0.1 M KCl. Excitation wavelength used are 404 nm for HPTS and 375 nm for PYTS to obtain the emission spectra.

Section 7: Fluorescence Intensity profiles of PYTS

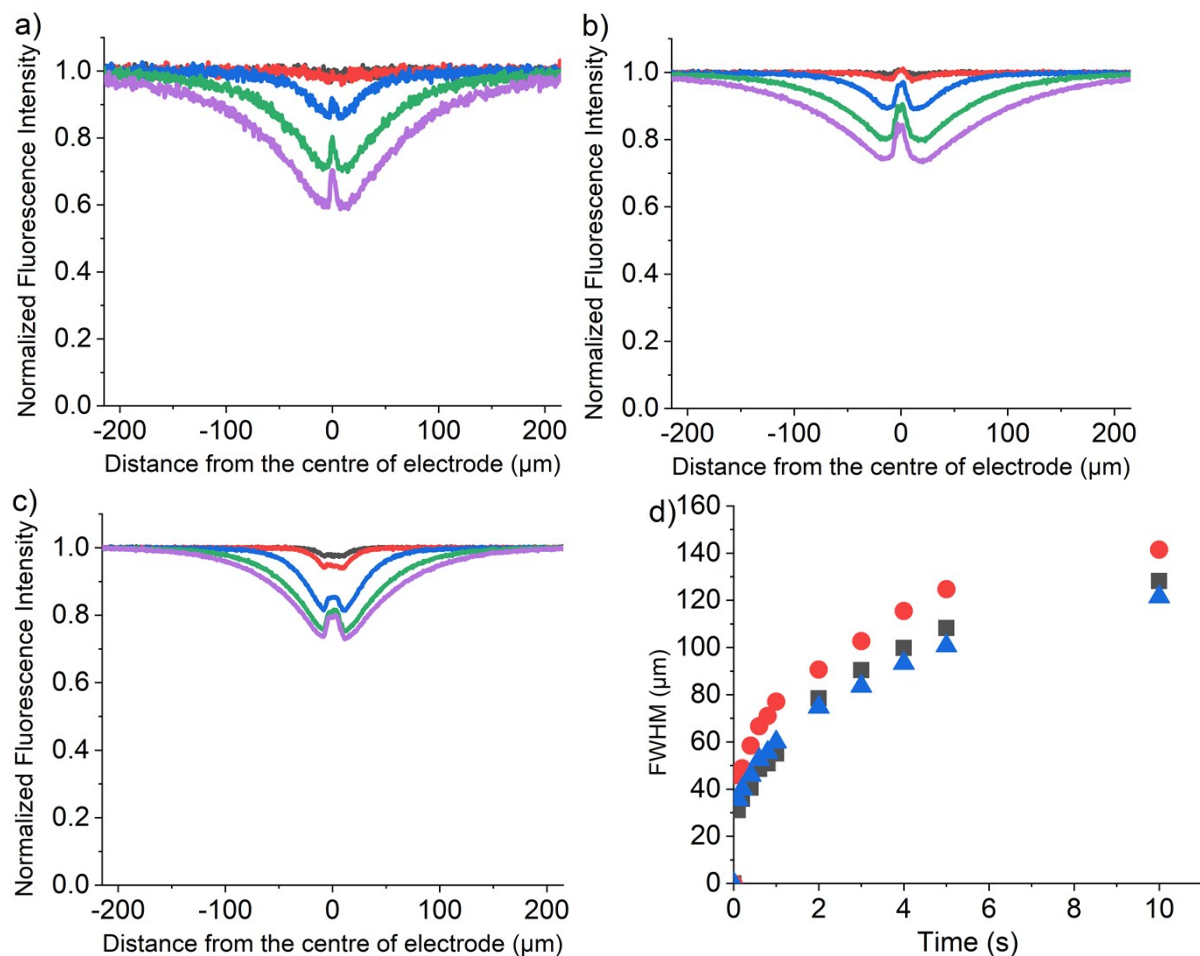


Figure S9: Relative Intensity profile recorded at $t = 0, 0.1, 1, 3$ and 5 s in a chronoamperometric experiment with a step potential of 2.3 V vs pseudo Ag wire reference electrode, measured as a function of distance perpendicular to the length of the cylindrical electrode (radius = 3.5 μm). The solution contains (a) 0.1 mM, (b) 1.0 mM, (c) 10 mM of PYTS with pH 7 phosphate buffer solution and 0.1 M KCl supporting electrolyte.

Time/s \ [HPTS]/mM	0	0.1	1.0	3.0	5.0
0.1					
1.0					

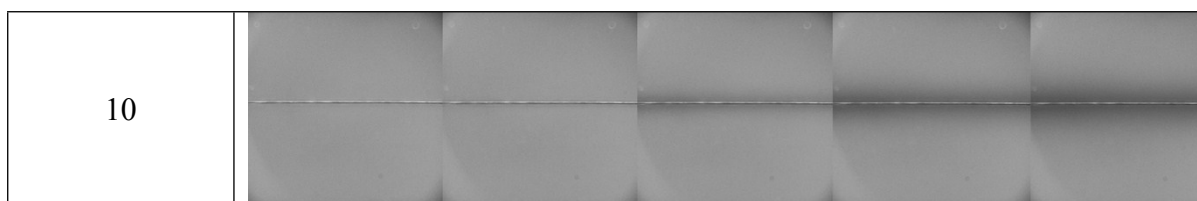


Figure S10: Fluorescence microscope images of a potentiostatically controlled carbon fibre wire electrode (radius = $3.5 \mu\text{m}$) at a step potential of 2.3 V (vs pseudo Ag wire) for 5 s . The solution contains 0.1 mM , 1.0 mM and 10 mM PYTS respectively with pH 7 phosphate buffer solution and 0.1 M KCl supporting electrolyte. Image series shows progression of the fluorescence turns off as a function of time.

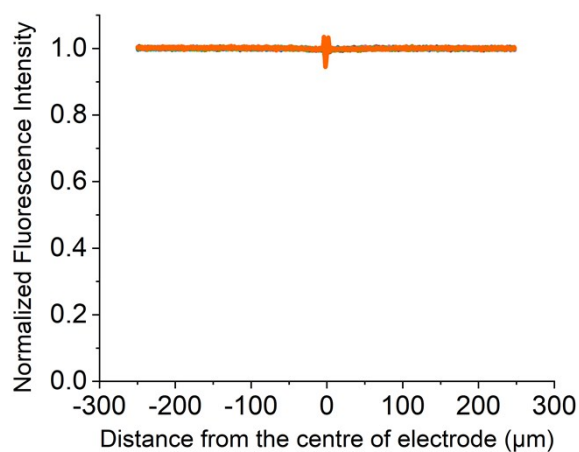


Figure S11: Intensity profile recorded at $t = 0$ to 5 s in a chronoamperometric experiment with a step potential of 1.4 V vs pseudo Ag wire reference electrode, measured as a function of distance perpendicular to the length of the cylindrical electrode (radius = $3.5 \mu\text{m}$). The solution contains 1.0 mM PYTS with pH 7 phosphate buffer solution and 0.1 M KCl supporting electrolyte.

Section 8: Fluorescence Intensity profiles of HPTS

In this section, plots of the fluorescence intensity profiles of HPTS with various concentrations as a function of time are provided with the fluorescence microscope images for both direct and mediated reactions.

Direct Reaction

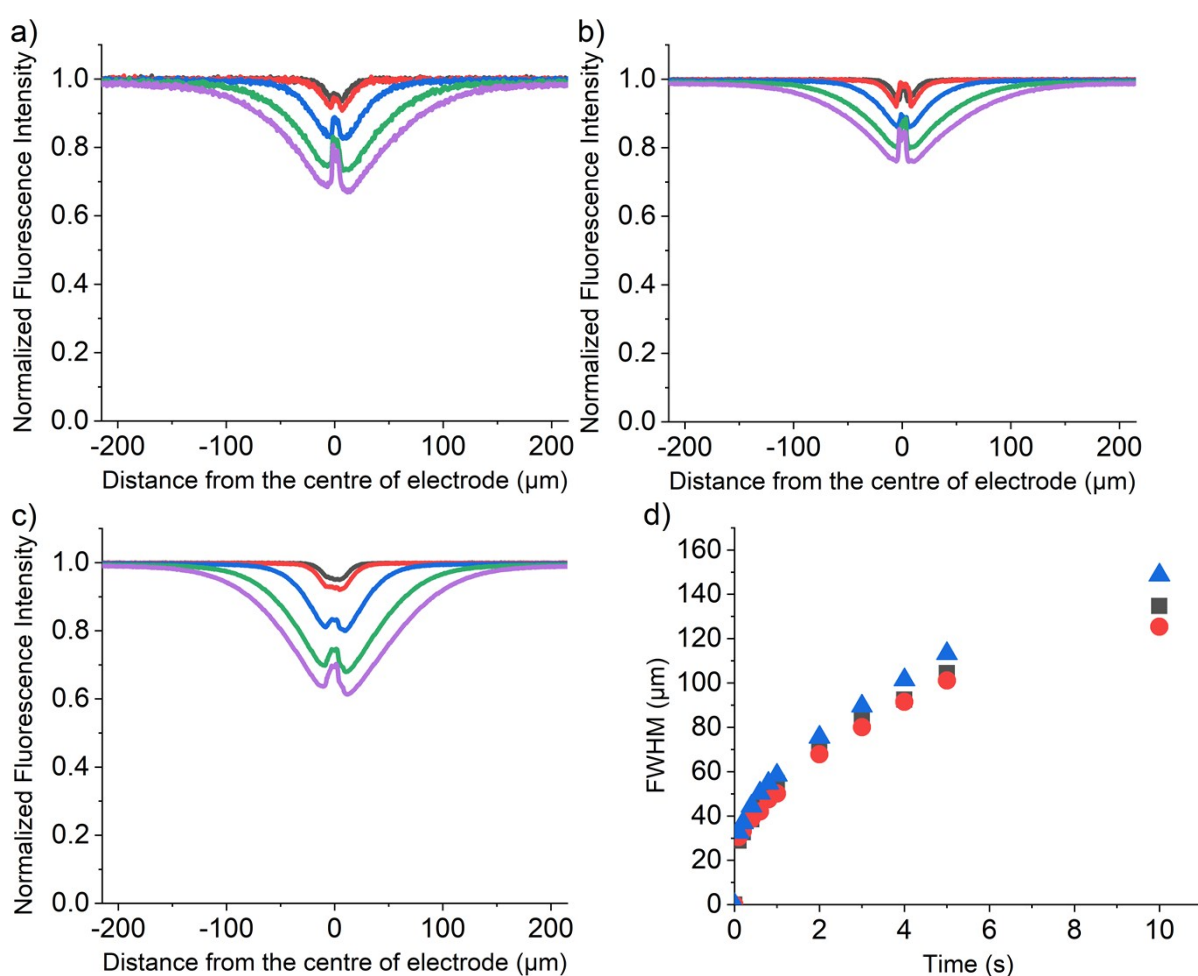


Figure S12: Plot of the variation in the relative fluorescence intensity profile recorded $t = 0, 0.1, 1, 3$ and 5 s in a chronoamperometric experiment with a step potential of 1.2 V vs pseudo Ag wire reference electrode, measured as a function of distance perpendicular to the length of the cylindrical electrode (radius = 3.5 μm). The solution contains a) 0.1 mM, b) 1 mM and c) 10 mM of HPTS with pH 7 phosphate buffer solution and 0.1 M KCl as supporting electrolyte. d) Plot of full-width half maximum of the concentration profiles of 0.1 mM (black), 1.0 mM (red) and 10 mM (blue) at $t = 0$ to 10 s.

Time/s \ [HPTS]/mM	0	0.1	1.0	3.0	5.0
0.1					
1.0					
10					

Figure S13: Fluorescence microscope images of the carbon fibre wire working electrode (radius = 3.5 μm) that is potentiostatically controlled at a potential of 1.2 V for 5 s (potentials measured against a silver pseudo reference electrode). The solution contains 0.1 mM, 1.0 mM and 10 mM HPTS respectively with pH 7 phosphate buffer solution and 0.1 M KCl supporting electrolyte. Image series show progression of the fluorescence turns off as a function of time.

Mediated Reaction

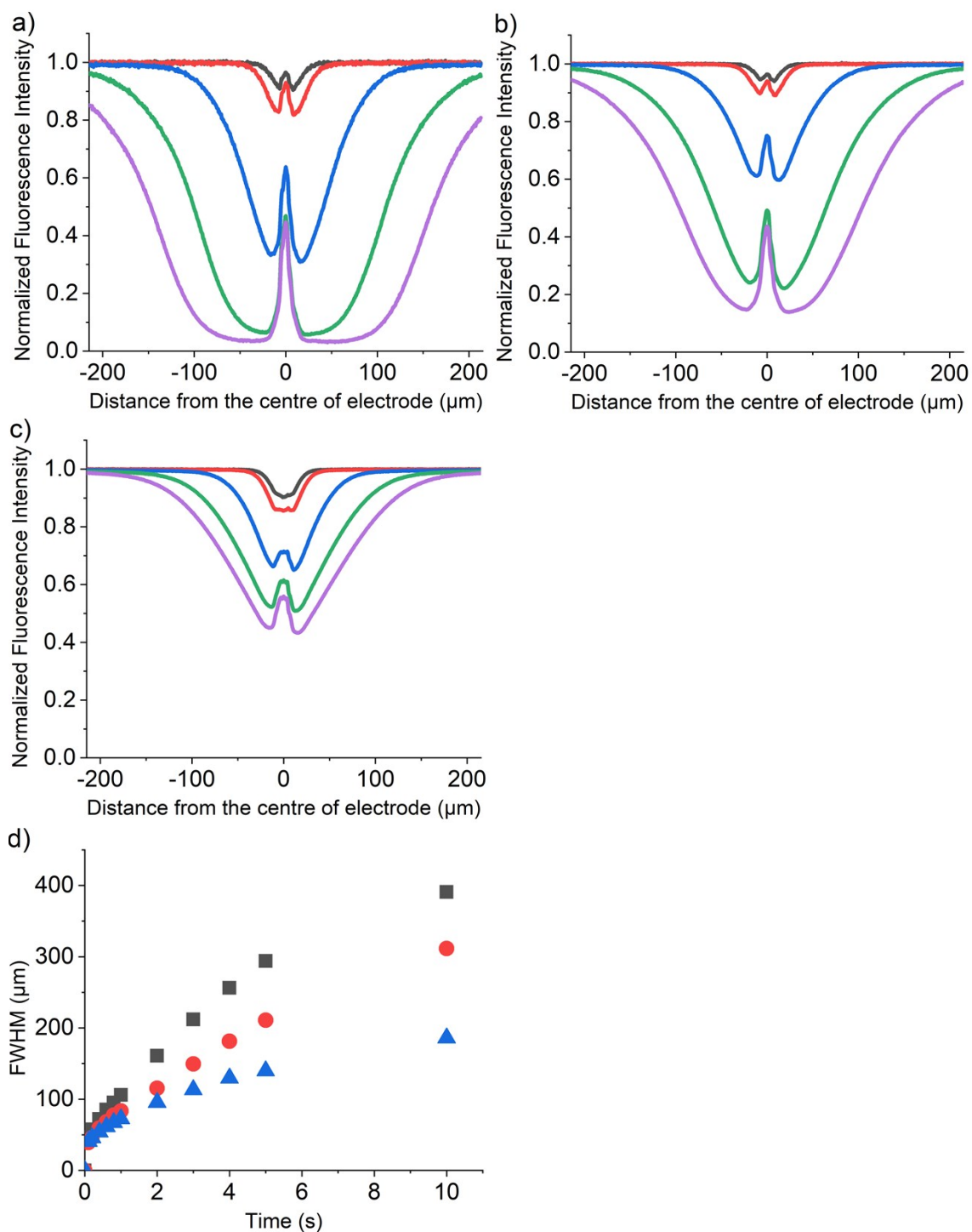


Figure S14: Plot of the variation in the relative fluorescence intensity profile recorded $t = 0, 0.1, 1, 3$ and 5 s in a chronoamperometric experiment with a step potential of 2.3 V vs pseudo Ag wire reference electrode, measured as a function of distance perpendicular to the length of the cylindrical electrode (radius = 3.5 μm). The solution contains a) 0.1 mM, b) 1 mM and c) 10 mM of HPTS with pH 7 phosphate buffer solution and 0.1 M KCl as supporting electrolyte. d) Plot of full-width half maximum of the concentration profiles of 0.1 mM (black), 1.0 mM (red) and 10 mM (blue) at $t = 0$ to 10 s.

Time/s \ [HPTS]/mM	0	0.1	1.0	3.0	5.0
0.1					
1.0					
10					

Figure S15: Fluorescence microscope images of a potentiostatically controlled carbon fibre wire electrode (radius = 3.5 μm) at a step potential of 2.3 V (vs pseudo Ag wire) for 5 s. The solution contains 0.1 mM, 1.0 mM and 10 mM HPTS respectively with pH 7 phosphate buffer solution and 0.1M KCl supporting electrolyte. Image series shows progression of the fluorescence turns off as a function of time.

On changing the electrolyte from 0.1 M KCl to 0.1 M KNO₃, at a high oxidative potential (+2.3 V), the fluorescence intensity profile was not as expected for mediated reaction. The depletion is much less than the one with KCl. Figure S13 depicts the comparison between the solution with and without 0.1 M KCl in 10 seconds. This suggests that electro-generated chlorine at 2.3V results in a mediated destruction of HPTS; this agrees with the UV-Vis evidence in SI Section 9 and 10.

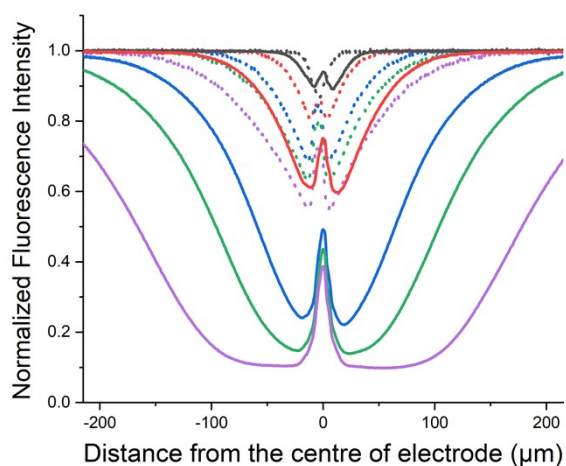


Figure S16: Plot of the variation in the normalized fluorescence intensity profile recorded $t = 0.1, 1, 3, 5$ and 10 s in a chronoamperometric experiment with a step potential of 2.3 V vs pseudo Ag wire reference electrode, measured as a function of distance perpendicular to the length of the cylindrical electrode (radius = 3.5 μm). The solution contains 1 mM HPTS with pH 7 phosphate buffer solution and 0.1 M KCl (Solid lines) or 0.1 M KNO_3 (Dotted lines).

References

1. Moon, P.; Spencer, D. E., *Field Theory Handbook: Including Coordinate Systems, Differential Equations and Their Solutions*; Springer, 2012.